SAND2017-2573PE

# General Model-Based Decomposition Framework for Polarimetric SAR Images

Stephen Dauphin

March 6, 2017

# Outline

# Introduction

With the growing number of model-based decompositions of polarimetric SAR images, with their various canonical scatter-types, there is a need for a **general model-based decomposition framework** to *implement* and *evaluate* these decompositions.

# Introduction

Geometry of Synthetic Aperture Radar (SAR)

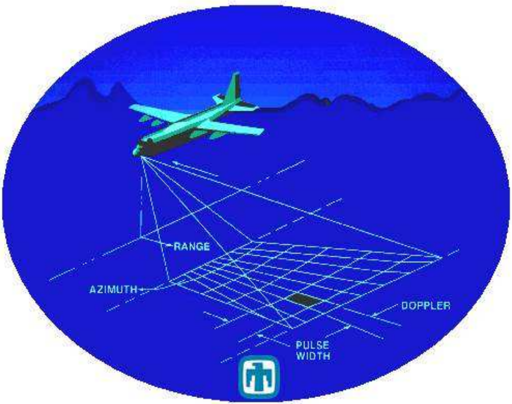

# Introduction

## Polarimetric SAR Diagram

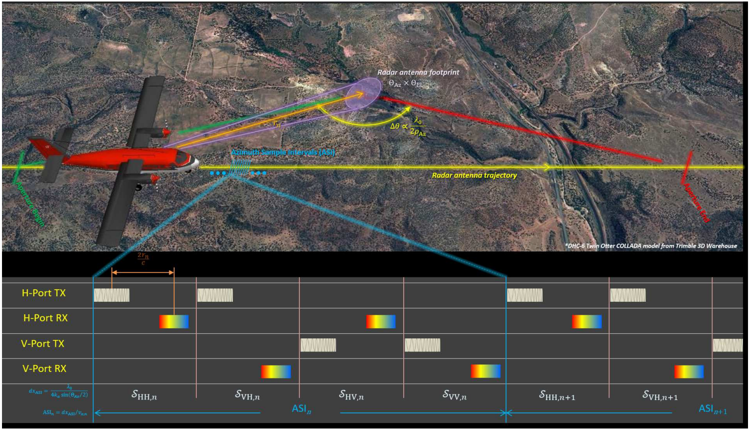

# Introduction

The collected phase histories are converted to 2D images that represent the scene's reflectivity
at each pixel using the method described in Jakowatz's text[1] .

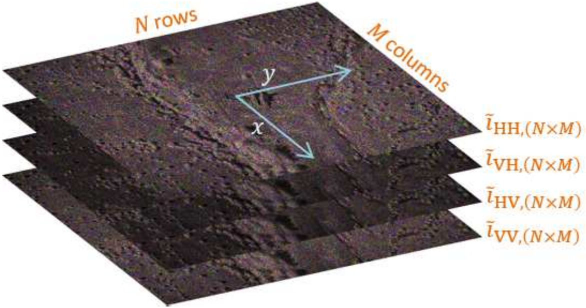


[1] **Jakowatz C.V., et al., Spotlight-mode Synthetic Aperture Radar, Springer, 1996.**

# Decomposition Building Blocks

The main building blocks for decompositions[2] are the Sinclair scattering matrix, $S$, and the Pauli feature vector, $k_P$, defined as

$$S = \begin{bmatrix} S_{\mathrm{HH}} & S_{\mathrm{HV}} \\ S_{\mathrm{VH}} & S_{\mathrm{VV}} \end{bmatrix} \qquad k_{\mathrm{P}} = \frac{1}{\sqrt{2}} \begin{bmatrix} S_{\mathrm{HH}} + S_{\mathrm{VV}} \\ S_{\mathrm{HH}} - S_{\mathrm{VV}} \\ 2S_{\mathrm{HV}} \end{bmatrix} \tag{1}$$

The corresponding coherency matrix $T$ is

$$\langle T \rangle = \langle k_{\mathrm{P}} k_{\mathrm{P}}^{\mathrm{H}} \rangle = \begin{bmatrix} T_{11} & T_{12} & T_{13} \\ T_{21} & T_{22} & T_{23} \\ T_{31} & T_{32} & T_{33} \end{bmatrix} \tag{2}$$

where $\langle \cdot \rangle$ denotes the spatial average

[2] **Lee J.**, **Pottier E.**, **Polarimetric Radar Imaging**, **CRC Press**, **2009**.

# Model-Based Decompositions

Model-based decompositions decompose the coherency matrix into contributions from canonical scatter-types.

$$\langle T \rangle = \sum_{i=1}^{n} f_i \left[ T \right]_i , \tag{3}$$

$f_i$ is scalar, and $\left[ T \right]_i$ represents the coherency matrix that describes the $i^{\mathrm{th}}$ canonical scatter-type.

# Model-Based Decompositions

## Freeman-Durden

The Freeman-Durden decomposition[3] assumes reflection symmetry and models the coherency matrix with three scatter-types.

$$\langle T \rangle = \begin{bmatrix} T_{11} & T_{12} & 0 \\ T_{21} & T_{22} & 0 \\ 0 & 0 & T_{33} \end{bmatrix} \tag{4}$$

$$\langle T \rangle = f_{\mathrm{s}} T_{\mathrm{s}} + f_{\mathrm{d}} T_{\mathrm{d}} + f_{\mathrm{v}} T_{\mathrm{v}} \tag{5}$$

s - Surface, d - Double-bounce, v - Volumetric

[3] **Freeman A., Durden, S. IEEE Geo. R.S. May 1998.**

# Model-Based Decompositions

## Freeman-Durden Surface Scattering

Scattering from a Bragg surface has the form

$$S_{\mathrm{s}} = \begin{bmatrix} R_{\mathrm{H}} & 0 \\ 0 & R_{\mathrm{V}} \end{bmatrix} \tag{6}$$

The reflection coefficients for horizontally and vertically polarized waves are given by

$$R_{\mathrm{H}} = \frac{\mu_{\mathrm{r}} \cos\phi - \sqrt{\varepsilon_{\mathrm{r}}\mu_{\mathrm{r}} - \sin^2\phi}}{\mu_{\mathrm{r}} \cos\phi + \sqrt{\varepsilon_{\mathrm{r}}\mu_{\mathrm{r}} - \sin^2\phi}} \tag{7}$$

$$R_{\mathrm{V}} = \frac{\varepsilon_{\mathrm{r}} \cos\phi - \sqrt{\varepsilon_{\mathrm{r}}\mu_{\mathrm{r}} - \sin^2\phi}}{\varepsilon_{\mathrm{r}} \cos\phi + \sqrt{\varepsilon_{\mathrm{r}}\mu_{\mathrm{r}} - \sin^2\phi}} \tag{8}$$

where $\phi$ is the local incidence angle, $\varepsilon_{\mathrm{r}}$ and $\mu_{\mathrm{r}}$ are the relative permittivity and permeability respectively .

# Model-Based Decompositions

## Freeman-Durden Surface Scattering

The associated Pauli feature vector and coherency matrix are

$$k_{\mathrm{P_s}} = \frac{1}{\sqrt{2}} \begin{bmatrix} R_{\mathrm{H}} + R_{\mathrm{V}} \\ R_{\mathrm{H}} - R_{\mathrm{V}} \\ 0 \end{bmatrix} \tag{9}$$

$$T_{\mathrm{s}} = \begin{bmatrix} \langle |R_{\mathrm{H}} + R_{\mathrm{V}}|^2 \rangle & \langle (R_{\mathrm{H}} + R_{\mathrm{V}})(R_{\mathrm{H}} - R_{\mathrm{V}})^* \rangle & 0 \\ \langle (R_{\mathrm{H}} + R_{\mathrm{V}})^* (R_{\mathrm{H}} - R_{\mathrm{V}}) \rangle & \langle |R_{\mathrm{H}} - R_{\mathrm{V}}|^2 \rangle & 0 \\ 0 & 0 & 0 \end{bmatrix}$$

$$T_{\mathrm{s}} = f_{\mathrm{s}} \begin{bmatrix} 1 & \beta^* & 0 \\ \beta & |\beta|^2 & 0 \\ 0 & 0 & 0 \end{bmatrix} \tag{10}$$

with $|\beta| < 1$ and $\beta \in \Re$

# Model-Based Decompositions

## Freeman-Durden Double-Bounce Scattering

Scattering from a dihedral is modeled by.

$$S_{\mathrm{d}} = \begin{bmatrix} e^{j2\gamma_{\mathrm{H}}} R_{\mathrm{WH}} R_{\mathrm{GH}} & 0 \\ 0 & e^{j2\gamma_{\mathrm{V}}} R_{\mathrm{WV}} R_{\mathrm{GV}} \end{bmatrix} \tag{11}$$

The horizontal and vertical reflection coefficients are

$$R_{i\mathrm{H}} = \frac{\cos\phi_i - \sqrt{\varepsilon_i - \sin^2\phi_i}}{\cos\phi_i + \sqrt{\varepsilon_i - \sin^2\phi_i}} \tag{12}$$

$$R_{i\mathrm{V}} = \frac{\varepsilon_i \cos\phi_i - \sqrt{\varepsilon_i - \sin^2\phi_i}}{\varepsilon_i \cos\phi_i + \sqrt{\varepsilon_i - \sin^2\phi_i}} \tag{13}$$

where $i \in \{\mathrm{W}, \mathrm{G}\}$ and the incidence angles $\phi_{\mathrm{G}} = \theta$ and $\phi_{\mathrm{W}} = \frac{\pi}{2} - \theta$.

# Model-Based Decompositions

## Freeman-Durden Double-Bounce Scattering

The corresponding coherency matrix is

$$T_{\mathrm{d}} = f_{\mathrm{d}} \begin{bmatrix} |\alpha|^2 & \alpha & 0 \\ \alpha^* & 1 & 0 \\ 0 & 0 & 0 \end{bmatrix} \tag{14}$$

where

$$\alpha = \frac{R_{\mathrm{WH}} R_{\mathrm{GH}} + e^{j\phi} R_{\mathrm{WV}} R_{\mathrm{GV}}}{R_{\mathrm{WH}} R_{\mathrm{GH}} - e^{j\phi} R_{\mathrm{WV}} R_{\mathrm{GV}}} \quad \text{and} \quad \phi = 2\gamma_{\mathrm{V}} - 2\gamma_{\mathrm{H}} \tag{15}$$

$\alpha$ is complex valued, and $|\alpha| < 1$.

# Model-Based Decompositions

## Freeman-Durden Volume Scattering

Volume scattering is modeled by a distribution of randomly oriented dipoles about the radar line of sight.

$$\langle T_{\text{vol}} \rangle = \int_0^{2\pi} T(\theta) p(\theta) \mathrm{d}\theta = \begin{bmatrix} a & d & e \\ d^* & b & f \\ e^* & f^* & c \end{bmatrix} \tag{16}$$

where the entries $a$, $b$, and $c$ are real, and $d$, $e$, and $f$ are complex.
For the case where $p(\theta)$ is uniform,

$$\langle T_{\text{v}} \rangle = \frac{1}{4} \begin{bmatrix} 2 & 0 & 0 \\ 0 & 1 & 0 \\ 0 & 0 & 1 \end{bmatrix} \tag{17}$$

# Model-Based Decompositions

## Freeman-Durden Assigning Powers

The Freeman-Durden Decomposition with these three models

$$\langle T \rangle = f_s \begin{bmatrix} 1 & \beta^* & 0 \\ \beta & |\beta|^2 & 0 \\ 0 & 0 & 0 \end{bmatrix} + f_d \begin{bmatrix} |\alpha|^2 & \alpha & 0 \\ \alpha^* & 1 & 0 \\ 0 & 0 & 0 \end{bmatrix} + \frac{f_v}{4} \begin{bmatrix} 2 & 0 & 0 \\ 0 & 1 & 0 \\ 0 & 0 & 1 \end{bmatrix} \tag{18}$$

$$T_{11} = f_s + f_d|\alpha|^2 + \frac{f_v}{2}$$

$$T_{22} = f_s|\beta|^2 + f_d + \frac{f_v}{4}$$

$$T_{33} = \frac{f_v}{4}$$

$$T_{12} = f_s\beta^* + f_d\alpha$$

# Model-Based Decompositions

## Freeman-Durden Assigning Powers

The power of a scatter-type is the trace.

$$P_{\mathrm{s}} = f_{\mathrm{s}} \left(1 + |\beta|^2\right) \tag{19}$$

$$P_{\mathrm{d}} = f_{\mathrm{d}} \left(1 + |\alpha|^2\right) \tag{20}$$

$$P_{\mathrm{v}} = f_{\mathrm{v}} \tag{21}$$

Several Issues

- Overestimation of Volume Power
- Volume model has priority
- Negative Powers
- Only handles reflection-symmetric case

# Model-Based Decompositions
## Yamaguchi

In order to address nonreflection symmetric case, Yamaguchi introduces a fourth scatter-type[4].

$$T_c = \frac{f_c}{2}\begin{bmatrix} 0 & 0 & 0 \\ 0 & 1 & \pm j \\ 0 & \mp j & 1 \end{bmatrix} \quad (22)$$

$$P_c = f_c \quad (23)$$

Several Issues

- Overestimation of Volume Power
- Helical and Volume models have priority
- Negative Powers
- Does not address $T_{13}$ or the real part of $T_{23}$

[4] **Yamaguchi Y., et al., IEEE Geo. R.S., 2005.**

# Model-Based Decompositions

## Line of Sight Rotation

Rotated dihedrals are misclassified as volume scattering. Therefore rotating the coherency matrix prior to the decomposition improves the decomposition[5].

$$\langle T(\theta)\rangle = R(\theta)\langle T\rangle R(\theta)^{*\mathrm{T}} \tag{24}$$

$$R_3(\theta) = \begin{bmatrix} 1 & 0 & 0 \\ 0 & \cos 2\theta & \sin 2\theta \\ 0 & -\sin 2\theta & \cos 2\theta \end{bmatrix} \tag{25}$$

$\theta$ is chosen to minimize the $T_{33}$ term

$$2\theta = \frac{1}{4}\left(\tan^{-1}\frac{2\mathrm{Re}\left(T_{23}\right)}{T_{22}-T_{33}} \pm n\pi\right) \quad n = 0, 1 \tag{26}$$

[5] **Lee J. S., Ainsworth T., IEEE Geo. R.S. Mar 2011.**

# Model-Based Decompositions
## G4U

Singh, et al.,[6] apply the rotation to the Yamaguchi decomp.

$$T_s(\theta) = f_s \begin{bmatrix} 1 & \beta^* \cos 2\theta & -\beta^* \sin 2\theta \\ \beta \cos 2\theta & |\beta|^2 \cos^2 2\theta & -\frac{1}{2}|\beta|^2 \sin 4\theta \\ -\beta \sin 2\theta & -\frac{1}{2}|\beta|^2 \sin 4\theta & |\beta|^2 \sin^2 2\theta \end{bmatrix} \quad (27)$$

$$T_d(\theta) = f_d \begin{bmatrix} |\alpha|^2 & \alpha \cos 2\theta & -\alpha \sin 2\theta \\ \alpha^* \cos 2\theta & \cos^2 2\theta & -\frac{1}{2} \sin 4\theta \\ -\alpha^* \sin 2\theta & -\frac{1}{2} \sin 4\theta & \sin^2 2\theta \end{bmatrix} \quad (28)$$

[6] **Singh G., et al., IEEE Geo. R. S. May 2013.**

# Model-Based Decompositions

## X-Bragg Surface

Schuler, et al., propose an X-Bragg surface model[7] that extends $T_\mathrm{s}$ to model surfaces rougher than SPM allows.

$$T_\mathrm{XB} = \int_0^{2\pi} T_\mathrm{s}(\theta)\, P(\theta) \mathrm{d}\theta. \tag{29}$$

$$P(\theta) = \frac{1}{\sigma\sqrt{2\pi}} \mathrm{e}^{-\theta^2/\left(2\sigma^2\right)}, \tag{30}$$

$$T_\mathrm{XB} = f_\mathrm{g} \begin{bmatrix} 1 & \beta^* \mathrm{e}^{-2\sigma^2} & 0 \\ \beta \mathrm{e}^{-2\sigma^2} & \frac{|\beta|^2}{2}\left(1 + \mathrm{e}^{-8\sigma^2}\right) & 0 \\ 0 & 0 & \frac{|\beta|^2}{2}\left(1 - \mathrm{e}^{-8\sigma^2}\right) \end{bmatrix} \tag{31}$$

[7] Schuler, et al., IEEE Geo. R.S. Mar. 2002.

# Model-Based Decompositions

## X-Bragg Surface

Hajnsek, et al., extend $T_s$ using a uniform pdf[8].

$$T_{XB} = \int_0^{2\pi} T_s(\theta)\, P(\theta) \mathrm{d}\theta. \tag{32}$$

$$P(\theta) = \begin{cases} \frac{1}{2\theta_1} & \theta| \leq \theta_1 \\ 0 & \text{otherwise} \end{cases} \quad \text{with} \quad 0 \leq \theta_1 \leq \frac{\pi}{2}, \tag{33}$$

$$T_{XB} = \begin{bmatrix} 1 & \beta^* \mathrm{sinc}(2\theta_1) & 0 \\ \beta \mathrm{sinc}(2\theta_1) & \frac{|\beta|^2}{2}(1 + \mathrm{sinc}(4\theta_1)) & 0 \\ 0 & 0 & \frac{|\beta|^2}{2}(1 - \mathrm{sinc}(4\theta_1)) \end{bmatrix}, \tag{34}$$

with $|\beta| \leq 1$.

[8] **Hajnsek I., IEEE Geo. R.S. Apr. 2003.**

# Model-Based Decompositions

## Adaptive Two-Component Decomposition

Huang, et al., adapt the Freeman II decomposition with Schuler's X-Bragg surface model and an improved volume model[9]

$$T_{\mathrm{v11}} = \frac{\sqrt{\pi}\Gamma\left(\frac{n+1}{2}\right)}{2\Gamma\left(\frac{n}{2}+1\right)} \, T_{\mathrm{v12}} = -\frac{n\sqrt{\pi}\Gamma\left(\frac{n+1}{2}\right)}{4\Gamma\left(\frac{n}{2}+2\right)} \tag{35}$$

$$T_{\mathrm{v33}} = \frac{\sqrt{\pi}\Gamma\left(\frac{n+3}{2}\right)}{\Gamma\left(\frac{n}{2}+3\right)} \, T_{\mathrm{v22}} = \frac{\left(n^2+2n+4\right)\sqrt{\pi}\Gamma\left(\frac{n+1}{2}\right)}{8\Gamma\left(\frac{n}{2}+3\right)} \tag{36}$$

$$A = \int_0^{\pi} \sin^n\theta \, d\theta = \int_{-\frac{\pi}{2}}^{\frac{\pi}{2}} \cos^n\theta \, d\theta = \frac{\sqrt{\pi}\Gamma\left(\frac{n+1}{2}\right)}{\Gamma\left(\frac{n}{2}+1\right)} \tag{37}$$

$$\Gamma(a) = \int_0^{\infty} \mathrm{e}^{-t} t^{a-1} \, dt. \tag{38}$$

[9] **Huang X., et al., IEEE Geo. R.S. Mar. 2016.**

# Model-Based Decompositions

## Chen

Chen, et al.[10], introduce a general decomposition for an observed coherency matrix $T$ is

$$T = T_{\mathrm{s}}(\theta_{\mathrm{odd}}) + T_{\mathrm{d}}(\theta_{\mathrm{dbl}}) + \langle T_{\mathrm{vol}} \rangle + T_{\mathrm{hel}} + T_{\mathrm{res}} \quad (39)$$

$T_{\mathrm{res}}$ is used to measure how well those models fit the observations. The smaller $T_{\mathrm{res}}$ is, the better the collection of models fits the data.

[10] **Chen S.W., et al., IEEE Geo. R.S., Mar 2014.**

# Model-Based Decompositions

## Chen

Using the canonical scattering models described in Chen's decomposition, the measured coherency matrix for a pixel is decomposed as follows:

$$\begin{bmatrix} T_{11} & T_{12} & T_{13} \\ T_{21} & T_{22} & T_{23} \\ T_{31} & T_{23} & T_{33} \end{bmatrix} =$$

$$f_{\mathrm{s}} \begin{bmatrix} 1 & \beta^* \cos 2\theta_{\mathrm{odd}} & -\beta^* \sin 2\theta_{\mathrm{odd}} \\ \beta \cos 2\theta_{\mathrm{odd}} & |\beta|^2 \cos^2 2\theta_{\mathrm{odd}} & -\frac{1}{2}|\beta|^2 \sin 4\theta_{\mathrm{odd}} \\ -\beta \sin 2\theta_{\mathrm{odd}} & -\frac{1}{2}|\beta|^2 \sin 4\theta_{\mathrm{odd}} & |\beta|^2 \sin^2 2\theta_{\mathrm{odd}} \end{bmatrix} + \cdots$$

$$f_{\mathrm{d}} \begin{bmatrix} |\alpha|^2 & \alpha \cos 2\theta_{\mathrm{dbl}} & -\alpha \sin 2\theta_{\mathrm{dbl}} \\ \alpha^* \cos 2\theta_{\mathrm{dbl}} & \cos^2 2\theta_{\mathrm{dbl}} & -\frac{1}{2} \sin 4\theta_{\mathrm{dbl}} \\ -\alpha^* \sin 2\theta_{\mathrm{dbl}} & -\frac{1}{2} \sin 4\theta_{\mathrm{dbl}} & \sin^2 2\theta_{\mathrm{dbl}} \end{bmatrix} + \cdots$$

$$f_{\mathrm{v}} \begin{bmatrix} a & d & e \\ d^* & b & f \\ e^* & f^* & c \end{bmatrix} + f_{\mathrm{c}} \begin{bmatrix} 0 & 0 & 0 \\ 0 & 1 & \pm j \\ 0 & \mp j & 1 \end{bmatrix} + \begin{bmatrix} T_{\mathrm{res11}} & T_{\mathrm{res12}} & T_{\mathrm{res13}} \\ T_{\mathrm{res21}} & T_{\mathrm{res22}} & T_{\mathrm{res23}} \\ T_{\mathrm{res31}} & T_{\mathrm{res23}} & T_{\mathrm{res33}} \end{bmatrix}$$

# Model-Based Decompositions
## Chen

Let $T_\mathrm{r}$ represent a vector that contains the real and imaginary elements that define $T_\mathrm{res}$. For model inversion, the optimization criterion is to minimize the square of the L2 norm of $T_\mathrm{r}$.

$$T_\mathrm{r} = \begin{bmatrix} T_\mathrm{res11} \\ T_\mathrm{res22} \\ T_\mathrm{res33} \\ \mathrm{Re}\left\{T_\mathrm{res12}\right\} \\ \mathrm{Re}\left\{T_\mathrm{res13}\right\} \\ \mathrm{Re}\left\{T_\mathrm{res23}\right\} \\ \mathrm{Im}\left\{T_\mathrm{res12}\right\} \\ \mathrm{Im}\left\{T_\mathrm{res13}\right\} \\ \mathrm{Im}\left\{T_\mathrm{res23}\right\} \end{bmatrix} \qquad ||T_\mathrm{r}||_2^2 = \sum_{i=1}^{9} |T_{\mathrm{r}(i)}|^2 \tag{40}$$

# Model-Based Decompositions

## Chen

The nine generic equations for $T_{\mathrm{r}(i)}$ are

$$
\begin{aligned}
T_{\mathrm{r}(1)} &= T_{11} - f_{\mathrm{d}}|\alpha|^2 - f_{\mathrm{s}} - af_{\mathrm{v}} \\
T_{\mathrm{r}(2)} &= T_{22} - f_{\mathrm{d}}\cos^2 2\theta_{\mathrm{dbl}} - f_{\mathrm{s}}|\beta|^2\cos^2 2\theta_{\mathrm{odd}} - bf_{\mathrm{v}} - \frac{f_{\mathrm{c}}}{2} \\
T_{\mathrm{r}(3)} &= T_{33} - f_{\mathrm{d}}\sin^2 2\theta_{\mathrm{dbl}} - f_{\mathrm{s}}|\beta|^2\sin^2 2\theta_{\mathrm{odd}} - cf_{\mathrm{v}} - \frac{f_{\mathrm{c}}}{2} \\
T_{\mathrm{r}(4)} &= \mathrm{Re}\{T_{12}\} - f_{\mathrm{v}}\mathrm{Re}\{d\} - f_{\mathrm{d}}\mathrm{Re}\{\alpha\}\cos 2\theta_{\mathrm{dbl}} - f_{\mathrm{s}}\mathrm{Re}\{\beta\}\cos 2\theta_{\mathrm{odd}} \\
T_{\mathrm{r}(5)} &= \mathrm{Re}\{T_{13}\} - f_{\mathrm{v}}\mathrm{Re}\{e\} + f_{\mathrm{d}}\mathrm{Re}\{\alpha\}\sin 2\theta_{\mathrm{dbl}} + f_{\mathrm{s}}\mathrm{Re}\{\beta\}\sin 2\theta_{\mathrm{odd}} \\
T_{\mathrm{r}(6)} &= \mathrm{Re}\{T_{23}\} - f_{\mathrm{v}}\mathrm{Re}\{f\} + \frac{f_{\mathrm{d}}}{2}\sin 4\theta_{\mathrm{dbl}} + \frac{f_{\mathrm{s}}}{2}|\beta|^2\sin 4\theta_{\mathrm{odd}} \\
T_{\mathrm{r}(7)} &= \mathrm{Im}\{T_{12}\} - f_{\mathrm{v}}\mathrm{Im}\{d\} - f_{\mathrm{d}}\mathrm{Im}\{\alpha\}\cos 2\theta_{\mathrm{dbl}} + f_{\mathrm{s}}\mathrm{Im}\{\beta\}\cos 2\theta_{\mathrm{odd}} \\
T_{\mathrm{r}(8)} &= \mathrm{Im}\{T_{13}\} - f_{\mathrm{v}}\mathrm{Im}\{e\} + f_{\mathrm{d}}\mathrm{Im}\{\alpha\}\sin 2\theta_{\mathrm{dbl}} - f_{\mathrm{s}}\mathrm{Im}\{\beta\}\sin 2\theta_{\mathrm{odd}} \\
T_{\mathrm{r}(9)} &= \mathrm{Im}\{T_{23}\} - f_{\mathrm{v}}\mathrm{Im}\{f\} - \frac{f_{\mathrm{c}}}{2} \qquad (41)
\end{aligned}
$$

# Model-Based Decompositions

## Chen

Let $F = \sum_{i=1}^{9} |T_{r(i)}|^2$

$$
\begin{aligned}
F &= \left(T_{11} - f_d|\alpha|^2 - f_s - af_v\right)^2 \\
&+ \left(T_{22} - f_d \cos^2 2\theta_{dbl} - f_s|\beta|^2 \cos^2 2\theta_{odd} - bf_v - \frac{f_c}{2}\right)^2 \\
&+ \left(T_{33} - f_d \sin^2 2\theta_{dbl} - f_s|\beta|^2 \sin^2 2\theta_{odd} - cf_v - \frac{f_c}{2}\right)^2 \\
&+ \left(\mathrm{Re}\left\{T_{12}\right\} - f_v\mathrm{Re}\left\{d\right\} - f_d\mathrm{Re}\left\{\alpha\right\} \cos 2\theta_{dbl} - f_s\mathrm{Re}\left\{\beta\right\} \cos 2\theta_{odd}\right)^2 \\
&+ \left(\mathrm{Re}\left\{T_{13}\right\} - f_v\mathrm{Re}\left\{e\right\} + f_d\mathrm{Re}\left\{\alpha\right\} \sin 2\theta_{dbl} + f_s\mathrm{Re}\left\{\beta\right\} \sin 2\theta_{odd}\right)^2 \\
&+ \left(\mathrm{Re}\left\{T_{23}\right\} - f_v\mathrm{Re}\left\{f\right\} + \frac{f_d}{2} \sin 4\theta_{dbl} + \frac{f_s}{2}|\beta|^2 \sin 4\theta_{odd}\right)^2 \\
&+ \left(\mathrm{Im}\left\{T_{12}\right\} - f_v\mathrm{Im}\left\{d\right\} - f_d\mathrm{Im}\left\{\alpha\right\} \cos 2\theta_{dbl} + f_s\mathrm{Im}\left\{\beta\right\} \cos 2\theta_{odd}\right)^2 \\
&+ \left(\mathrm{Im}\left\{T_{13}\right\} - f_v\mathrm{Im}\left\{e\right\} + f_d\mathrm{Im}\left\{\alpha\right\} \sin 2\theta_{dbl} - f_s\mathrm{Im}\left\{\beta\right\} \sin 2\theta_{odd}\right)^2 \\
&+ \left(\mathrm{Im}\left\{T_{23}\right\} - f_v\mathrm{Im}\left\{f\right\} - \frac{f_c}{2}\right)^2 \qquad (42)
\end{aligned}
$$

# Model-Based Decompositions
## Chen

The objective function (27) is minimized with the following constraints:

$$0 \leq f_{\mathrm{v}}, f_{\mathrm{d}}, f_{\mathrm{s}} \leq \mathrm{Tr}\left\{T\right\} \quad 0 \leq f_{\mathrm{c}} \leq 2|\mathrm{Im}\left(T_{23}\right)| \tag{43}$$

$$-\frac{\pi}{4} \leq \theta_{\mathrm{dbl}}, \theta_{\mathrm{odd}} \leq \frac{\pi}{4} \quad |\beta|, |\alpha| < 1 \tag{44}$$

where $\mathrm{Tr}\left\{T\right\} = T_{11} + T_{22} + T_{33}$ is the trace of the measured coherency matrix.

# Model-Based Decompositions

## Decomposition Implementation

Minimizing (27) is a little tricky.

- MATLAB's `fmincon` function

[11] **Boyd S.**, **Vandenberghe L.**, **Convex Optimization**, **Cambridge University Press**, **2004**.

# Model-Based Decompositions

## Decomposition Implementation

Minimizing (27) is a little tricky.

- MATLAB's `fmincon` function
- Newton's Method

[11] **Boyd S.**, **Vandenberghe L.**, **Convex Optimization**, **Cambridge University Press**, **2004**.

# Model-Based Decompositions

## Decomposition Implementation

Minimizing (27) is a little tricky.

- MATLAB's `fmincon` function
- Newton's Method

Bad results are due to the function being nonconvex!

[11] **Boyd S.**, **Vandenberghe L.**, **Convex Optimization**, **Cambridge University Press**, **2004**.

# Model-Based Decompositions

## Decomposition Implementation

Minimizing (27) is a little tricky.

- MATLAB's `fmincon` function
- Newton's Method

Bad results are due to the function being nonconvex!

A function is convex[11] if

$$\forall t \in [0,1], \forall \underline{\boldsymbol{x}}_1, \underline{\boldsymbol{x}}_2 \in D$$
$$F\left(t\underline{\boldsymbol{x}}_1 + (1-t)\,\underline{\boldsymbol{x}}_2\right) \leq tF\left(\underline{\boldsymbol{x}}_1\right) + (1-t)\,F\left(\underline{\boldsymbol{x}}_2\right) \qquad (45)$$

[11] **Boyd S., Vandenberghe L., Convex Optimization, Cambridge University Press, 2004.**

# Model-Based Decompositions

## Decomposition Implementation

Define $\underline{\boldsymbol{x}}_1$ and $\underline{\boldsymbol{x}}_2$ as follows:

$$\begin{bmatrix} f_\mathrm{s} \\ f_\mathrm{d} \\ f_\mathrm{v} \\ f_\mathrm{c} \\ \theta_\mathrm{odd} \\ \theta_\mathrm{dbl} \\ \mathbf{Re}\left\{\alpha\right\} \\ \mathbf{Im}\left\{\alpha\right\} \\ \mathbf{Re}\left\{\beta\right\} \end{bmatrix} \qquad \underline{\boldsymbol{x}}_1 = \begin{bmatrix} 200.9667 \\ 0 \\ 0 \\ 0 \\ 0.5620 \\ 0 \\ 0 \\ 0 \\ -0.2550 \end{bmatrix} \qquad \underline{\boldsymbol{x}}_2 = \begin{bmatrix} 211.5955 \\ 0 \\ 0 \\ 0 \\ -0.7021 \\ 0 \\ 0 \\ 0 \\ -0.5247 \end{bmatrix}. \tag{46}$$

# Model-Based Decompositions

## Decomposition Implementation

These values for $\underline{\boldsymbol{x}}_1$ and $\underline{\boldsymbol{x}}_2$ represent two different points within the bounds from (43). Therefore, their residual can be formed with the same objective function with the measured coherency values

$$\langle \boldsymbol{T} \rangle = \begin{bmatrix} 690.86 & 734.16 + 97.64i & 120.17 + 83.50i \\ 734.16 - 97.64i & 814.94 & 141.11 + 80.19i \\ 120.17 - 83.50i & 141.11 - 80.19i & 35.11 \end{bmatrix}. \tag{47}$$

# Model-Based Decompositions

## Decomposition Implementation

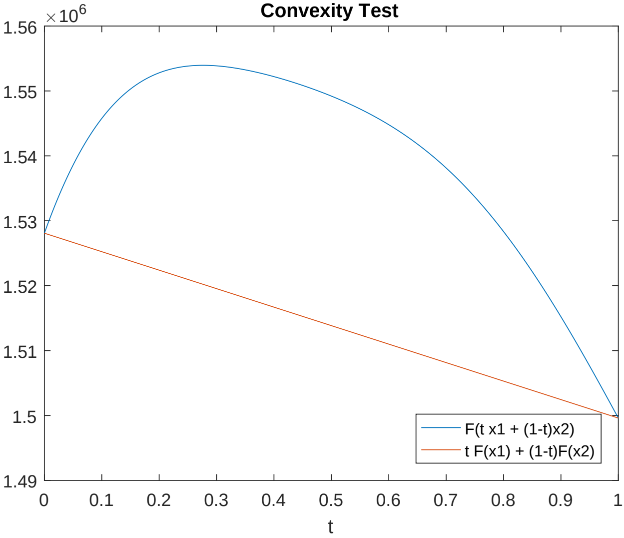

# Model-Based Decompositions

## Decomposition Implementation

The method of steepest descent is applied to parameters, $x_0$, that are supplied by the $G4U$ decomp.
Set

$$x_1 = -\lambda \nabla F(x_0) + x_0 \tag{48}$$

with $\lambda = 1$.
$x_1$ must satisfy the following:

- $x_1$ satisfies the constraints
- The residual at $x_1$ is lower than $x_0$, $F(x_1) < F(x_0)$

Reduce $\lambda$ until both conditions are met.

# Model-Based Decompositions

## Decomposition Implementation

Steepest Descent Algorithm:

- Set $x_0, F(x_0), \nabla F(x_0)$ at each pixel.
- Set $x_1 = -\nabla F(x_0) + x_0$
- For pixels that do not satisfy both conditions, divide $\lambda$ by 10 and reset $x_1$
- Continue to adjust $\lambda$ and reset $x_1$ until a desired tolerance is reached.
- Set $x_0 = x_1$ and rerun the previous 4 steps.
- Continue iterations until a minimum (local) is reached.

# General Model-Based Decomposition Framework

Chen's decomposition can be *expanded* to be a **framework** for a whole family of model-based decompositions.

Scatter-types can be interchanged depending on the situation and the residual provides a way evaluate how well the scatter-types model the data.

$$\langle T \rangle = \sum_{i=1}^{n} (f_i T_i) + T_{\mathrm{res}} \tag{49}$$

# General Model-Based Decomposition Framework

## Linear Independence for Scatter-Types

The scatter-types in this framework must be linearly independent.
If not, then

$$f_\mathrm{a} T_\mathrm{a} = f_\mathrm{b} T_\mathrm{b} + f_\mathrm{c} T_\mathrm{c} + \dots \tag{50}$$

which forces $P_\mathrm{a} = 0$ and $P_\mathrm{a} \neq 0$
. . . which is bad.

Therefore, care must be taken to ensure that the scatter-types being used are linearly independent.

# General Model-Based Decomposition Framework

## Number of Parameters

Chen, et al., claim that the maximum number of unknown parameters should be limited to nine[12].

[12] **Chen S.W., et al., IEEE Geo. R.S., Mar 2014.**

# General Model-Based Decomposition Framework

## Number of Parameters

Chen, et al., claim that the maximum number of unknown parameters should be limited to nine[12].

THIS IS FALSE!!

[12] **Chen S.W., et al., IEEE Geo. R.S., Mar 2014.**

Chen, et al., claim that the maximum number of unknown parameters should be limited to nine[12].

**THIS IS FALSE!!**

As long as the scatter-types are linearly independent, any number of parameters are allowed.

[12] **Chen S.W., et al., IEEE Geo. R.S., Mar 2014.**

# General Model-Based Decomposition Framework

## Example: Complex $\beta$

Compare the Chen decomposition with a new decomposition that switches in a surface model that includes a complex $\beta$.

# General Model-Based Decomposition Framework

## Example: Complex $\beta$

Compare the Chen decomposition with a new decomposition that switches in a surface model that includes a complex $\beta$.

- Run Chen decomposition.

# General Model-Based Decomposition Framework

## Example: Complex $\beta$

Compare the Chen decomposition with a new decomposition that switches in a surface model that includes a complex $\beta$.

- Run Chen decomposition.
- Run new decomposition with complex beta.

# General Model-Based Decomposition Framework

## Example: Complex $\beta$

Compare the Chen decomposition with a new decomposition that switches in a surface model that includes a complex $\beta$.

- Run Chen decomposition.
- Run new decomposition with complex beta.
- Compare the residual values.

# Results

Chen image of Gibson Blvd. on KAFB.

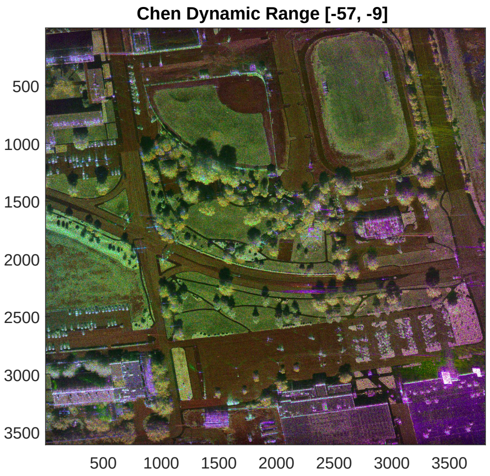

# Results

ImBeta image of Gibson Blvd. on KAFB.

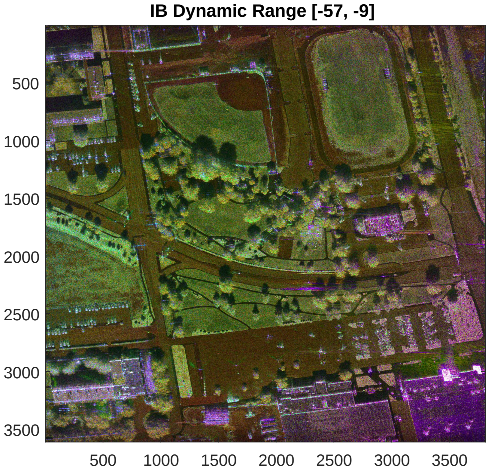

# Results

Pixels that improve the Chen with the ImBeta

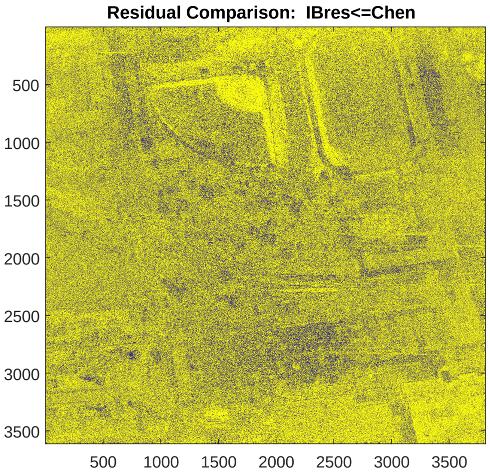

# Results

Chen chip of Gibson Blvd. on KAFB.

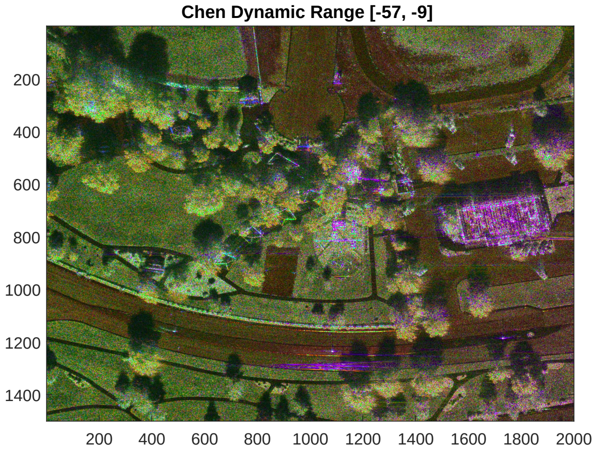

# Results

ImBeta chip of Gibson Blvd. on KAFB.

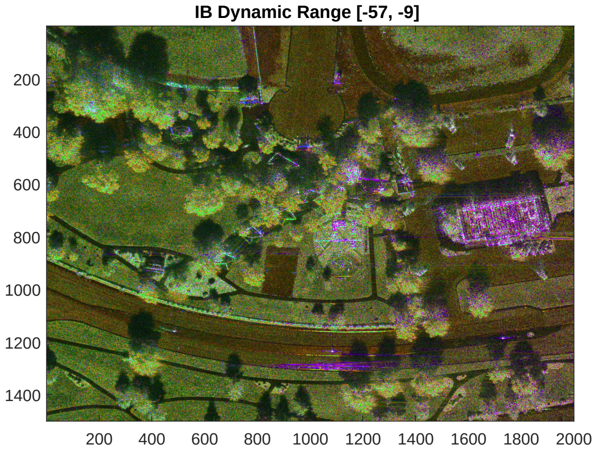

# Results

Pixels that improve the Chen with the ImBeta

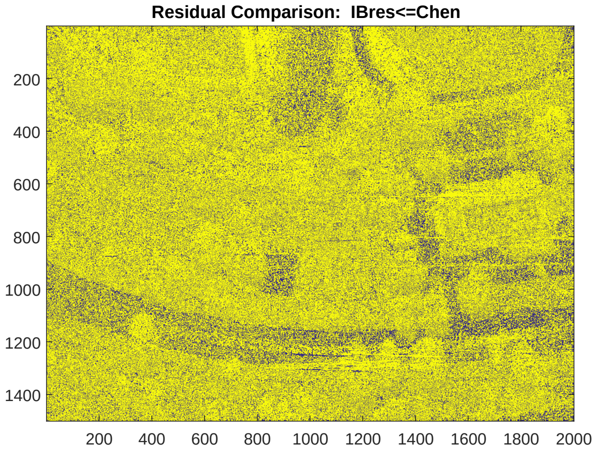

# Results

The sum of the residuals across the image are

| Decomp | Total Residual |
|---|---|
| Freeman-Durden | 5728273 |
| G4U | 2802118 |
| Chen | 1176796 |
| ImBeta | 1150272 |

# Application

Terrain Classification[13].

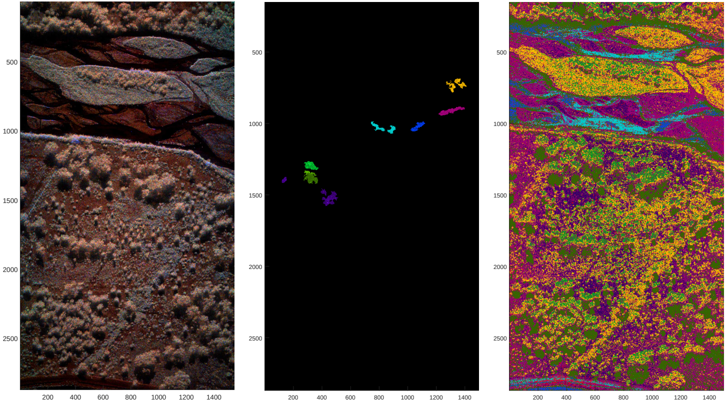


[13] **Dauphin S., et al., 48th Asilomar Conference, Nov. 2014.**

# Conclusion

With this research effort, I have

- developed a general framework that encompasses all the scatter-types of existing decompositions.

# Conclusion

With this research effort, I have

- developed a general framework that encompasses all the scatter-types of existing decompositions.
- provided a method for evaluating how good a collection of scatter-types is by comparing residuals.

# Conclusion

With this research effort, I have

- developed a general framework that encompasses all the scatter-types of existing decompositions.
- provided a method for evaluating how good a collection of scatter-types is by comparing residuals.
- developed a notion of linear independence of scatter-types.

# Conclusion

With this research effort, I have

- developed a general framework that encompasses all the scatter-types of existing decompositions.
- provided a method for evaluating how good a collection of scatter-types is by comparing residuals.
- developed a notion of linear independence of scatter-types.
- shown that the existing belief that decompositions are limited to 9 parameters is false, which enables new combinations of scatter-types to create new decompositions.

# Conclusion

With this research effort, I have

- developed a general framework that encompasses all the scatter-types of existing decompositions.
- provided a method for evaluating how good a collection of scatter-types is by comparing residuals.
- developed a notion of linear independence of scatter-types.
- shown that the existing belief that decompositions are limited to 9 parameters is false, which enables new combinations of scatter-types to create new decompositions.
- given an example of a new decomposition (ImBeta) that has a lower residual than the other existing decompositions.

# Conclusion

With this research effort, I have

- developed a general framework that encompasses all the scatter-types of existing decompositions.
- provided a method for evaluating how good a collection of scatter-types is by comparing residuals.
- developed a notion of linear independence of scatter-types.
- shown that the existing belief that decompositions are limited to 9 parameters is false, which enables new combinations of scatter-types to create new decompositions.
- given an example of a new decomposition (ImBeta) that has a lower residual than the other existing decompositions.
- given an example of the utility of model-based decompositions to classify terrain.

# References I


- C. V. Jakowatz Jr., D. E. Wahl, P. E. Eichel, D. C. Ghiglia, and P. A. Thompson, *Spotlight-mode Synthetic Aperture Radar: A Signal Processing Approach*. Springer, 1996.
- J. Lee and E. Pottier, *Polarimetric Radar Imaging: From Basics to Applications*. CRC Press, 2002.
- A. Freeman and S. Durden, "A three-component scattering model for polarimetric SAR data," *Geoscience and Remote Sensing, IEEE Transactions on*, vol. 36, no. 3, pp. 963–973, 1998, ISSN: 0196-2892. DOI: 10.1109/36.673687.

# References II

Y. Yamaguchi, T. Moriyama, M. Ishido, and H. Yamada, "Four-component scattering model for polarimetric SAR image decomposition," *Geoscience and Remote Sensing, IEEE Transactions on*, vol. 43, no. 8, pp. 1699–1706, 2005.

J.-S. Lee and T. Ainsworth, "The effect of orientation angle compensation on coherency matrix and polarimetric target decompositions," *Geoscience and Remote Sensing, IEEE Transactions on*, vol. 49, no. 1, pp. 53–64, 2011, ISSN: 0196-2892. DOI: 10.1109/TGRS.2010.2048333.

# References III


G. Singh, Y. Yamaguchi, and S.-E. Park, "General four-component scattering power decomposition with unitary transformation of coherency matrix," *Geoscience and Remote Sensing, IEEE Transactions on*, vol. 51, no. 5, pp. 3014–3022, 2013, ISSN: 0196-2892. DOI: 10.1109/TGRS.2012.2212446.

D. L. Schuler, J.-S. Lee, D. Kasilingam, and G. Nesti, "Surface roughness and slope measurements using polarimetric sar data," *IEEE Transactions on Geoscience and Remote Sensing*, vol. 40, no. 3, pp. 687–698, 2002, ISSN: 0196-2892. DOI: 10.1109/TGRS.2002.1000328.

# References IV


X. Huang, J. Wang, and J. Shang, "An adaptive two-component model-based decomposition on soil moisture estimation for c-band radarsat-2 imagery over wheat fields at early growing stages," *IEEE Geoscience and Remote Sensing Letters*, vol. 13, no. 3, pp. 414–418, 2016, ISSN: 1545-598X. DOI: 10.1109/LGRS.2016.2517082.

S.-W. Chen, X. song Wang, S.-P. Xiao, and M. Sato, "General polarimetric model-based decomposition for coherency matrix," *IEEE Transactions on Geoscience and Remote Sensing*, vol. 52, no. 3, pp. 1843–1855, 2014, ISSN: 0196-2892. DOI: 10.1109/TGRS.2013.2255615.

S. Boyd and L. Vandenberghe, *Convex Optimization*. Cambridge University Press, 2004.

# References V

S. Dauphin, R. Derek West, R. Riley, and K. M. Simonson, "Semi-supervised classification of terrain features in polarimetric sar images using h/a/alpha; and the general four-component scattering power decompositions," in *Signals, Systems and Computers, 2014 48th Asilomar Conference on*, 2014, pp. 167–171. DOI: 10.1109/ACSSC.2014.7094420.